Observation of Spontaneous Magnetization in the Layered Perovskite Ferromagnet, (*p*-Chloroanilinium)$_2$CuBr$_4$

Taketoshi Sekine, Tsunehisa Okuno, and Kunio Awaga*

Department of Basic Science, Graduate School of Arts and Sciences, The University of Tokyo, Komaba, Meguro, Tokyo 153, Japan

Received June 27, 1997

The crystal structure and magnetic properties of the layered perovskite, (*p*-chloroanilinium)$_2$CuBr$_4$ (**1**) have been investigated. The crystal of **1** belongs to the orthorhombic *Pbca* space group [$a = 7.551(2)$ Å, $b = 32.082(10)$ Å, $c = 7.879(2)$ Å, and $Z = 4$], which is typical of the material family. The temperature dependence of the ac susceptibility ($\chi_{ac} = (\partial M/\partial H)$) of a polycrystalline sample shows magnetic ordering at 15 K with an abrupt increase of the value. In the ordered state, the field dependence of χ_{ac}, namely the differential susceptibility, and the dc magnetization indicate a hysteresis loop of the magnetization, which can be ascribed to the presence of spontaneous magnetization. Furthermore, single-crystal magnetic measurements indicate that the magnetic properties of **1** are quite anisotropic. When the field is along the *b* axis (perpendicular to the inorganic layer), the field dependence of χ_{ac} shows the hysteresis behavior, as observed for the polycrystals, but when it is parallel to the *a* axis (parallel to the layer), χ_{ac} shows metamagnetic transitions. The observed anisotropy can be understood in terms of a magnetic easy axis parallel to the *a* axis, an antiferromagnetic interlayer interaction, and a spin canting which produces spontaneous magnetization along the *b* axis.

1. Introduction

For the past decades, magnetic properties of transition-metal layered materials have been studied extensively, because they are good examples of two-dimensional magnetic systems.[1] While ideal 2D Heisenberg spin systems are theoretically predicted not to show magnetic ordering at any finite temperature,[2−4] real 2D materials show various magnetic transitions, such as the Kosterliz−Thouless transition.[5,6] The magnetic ground states and the transition temperatures of the 2D layered systems are governed by the intralayer interaction and the characteristic minor factors, such as the interlayer interaction and the magnetic anisotropy.[1] What is described in this report is an example that such minor factors bring about a crucial difference in the magnetic ordering among three isostructural 2D ferromagnets.

Compounds of the type $(RNH_3)_2CuX_4$, where R is an organic molecule and X is Cl or Br, have been known as two-dimensional (2D) ferromagnets with T_c values of 10−15 K.[1,7−10] The compounds also attracted recent interest as a related material of the high T_c superconductors and as an organic/inorganic hybrid layered system. They crystallize in a layered perovskite structure, consisting of isolated layers of corner-sharing CuX_6 octahedra, sandwiched by the organic cations.[8,11,12] The structure of the CuX_4 layer is schematically shown in Figure 1. It is governed by the cooperative Jahn−Teller effect: each octahedron is prolonged along the Jahn−Teller *z* axis that lies in the CuX plane and has nearly-orthogonal relations with the neighbors. The intralayer magnetic interaction is ferromagnetic, because of the orthogonal relation between the magnetic $d_{x^2-y^2}$ orbitals.[13] The interlayer magnetic coupling is much weaker than the intralayer interaction and is usually antiferromagnetic. The magnetic moments are, therefore, canceled out with each other, so there is no spontaneous magnetization in the ground state. A few compounds in the series have been reported to possess a ferromagnetic interlayer interaction.[10,14] However, there has been no observation of spontaneous magnetization as a nonzero remnant magnetization so far, presumably because the interlayer interaction would be too weak to make the magnetic hysteresis loop observable.[10,14]

In this report we describe the crystal structure and magnetic properties of (*p*-chloroanilinium)$_2$CuBr$_4$ (**1**), comparing with those of the isostructural copper chloride derivatives, (*p*-chloroanilinium)$_2$CuCl$_4$ (**2**) and (*p*-nitroanilinium)$_2$CuCl$_4$ (**3**).

2. Experimental Section

The crystals of compound **1** were prepared according to the method reported by Ishikawa et al.[15] To an alcoholic solution of *p*-chloroanilinium bromide and hydrobromic acid was slowly added a hydrobromic solution of $CuBr_2$. The dark-violet crystalline precipitate was filtered and washed with hexane. Chemical analysis, calcd (found) for $C_{12}H_{14}N_2Br_4Cl_2Cu$: C, 22.51 (22.42); H, 2.20 (2.34); N, 4.38 (4.38); Br, 49.92 (50.09); Cl, 11.07 (11.20).

(1) Jongh, L. J. d.; Miedema, A. R. *Adv. Phys.* **1974**, *23*, 1.
(2) Mermin, N. D.; Wagner, H. *Phys. Rev. Lett.* **1966**, *17*, 1133.
(3) Hohenberg, P. C. *Phys. Rev.* **1967**, *158*, 383.
(4) Mermin, N. D. *Phys. Rev.* **1968**, *176*, 176.
(5) Kosterlitz, J. M.; Thouless, D. J. *J. Phys.* **1972**, *C5*, 124.
(6) Kosterlitz, J. M.; Thouless, D. J. *J. Phys.* **1973**, *C6*, 1181.
(7) Willett, R. D. In *Magneto-Structual Correlations in Exchange Coupled Systems;* Willett, R. D., Gatteschi, D., Kahn, O., Eds.; D. Reidel Publishing Company: Dordrecht, The Netherlands, 1985; p 269.
(8) Willett, R.; Place, H.; Middleton, M. *J. Am. Chem. Soc.* **1988**, *110*, 8639.
(9) Smith, D. W. *Coord. Chem. Rev.* **1976**, *21*, 93.
(10) Steijger, J. J. M.; Frikkee, E.; Jongh, L. J. d.; Huiskamp, W. D. *Physica* **1984**, *B123*, 271.
(11) Steadman, J. P.; Willett, R. D. *Inorg. Chem. Acta* **1970**, *4*, 367.
(12) Larsen, K. P. *Acta Chem. Scand.* **1974**, *A28*, 194.
(13) Kugel, K. I.; Khomskii, D. I. *Sov. Phys. Usp.* **1982**, *25*, 231.
(14) Jongh, L. J. d.; Amstel, W. D. v.; Miedema, A. R. *Physica* **1972**, *58*, 277.
(15) Ishikawa, J.; Asaji, T.; Nakamura, D. *J. Magn. Reson.* **1982**, *51*, 95.

S0020-1669(97)00793-3 CCC: $15.00
Published on Web 04/03/1998

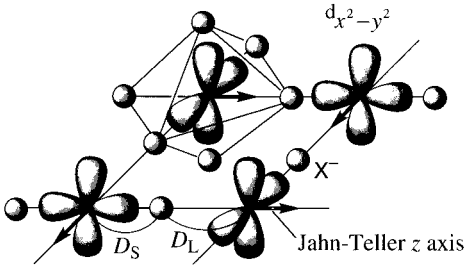

Figure 1. The structure of the CuX_4 layer.

Table 1. The Crystal Data for **1**

formula	$C_{12}H_{14}N_2Cl_2CuBr_4$
fw	640.32
cryst syst	orthorhombic
space group	*Pbca* (No. 61)
a/Å	7.551(2)
b/Å	32.082(10)
c/Å	7.879(2)
V/Å^3	1908.8(9)
Z	4
ρ(calc)/g cm^{-3}	2.23
μ/cm^{-1}	103.3
2θ range/deg	4.0−55
R^a	0.0842
$R_w{}^b$	0.104

[a] $R = \sum||F_o| - |F_c||/\sum|F_o|$. [b] $R_w = \{\sum w(|F_o| - |F_c|)^2/\sum w|F_o|^2\}^{1/2}$, $w = 1/(\sigma(F_o)^2 + 0.0020F_o^2)$.

X-ray diffraction data of **1** was collected on a Rigaku AFC-5 automatic four-circle diffractometer with graphite-monochromatized Mo $K\alpha$ radiation at 293 K. The diameter of the incident beam collimator was 1.0 mm, the crystal-to-detector distance was 258 mm, and the detector aperture was 9.0 × 13.0 (horizontal × vertical). The unit cell parameters were derived by least-squares refinements of the setting angles of 25 representative reflections in the range $20° < 2\theta < 25°$. During the data collection, the intensities of three reflections were monitored as a check on crystal stability, and no loss of intensity was found. An empirical absorption correction based on azimuthal scans of several reflections using UNICS III[16] was applied. The transmission factors ranged from 0.25 to 1.00. Lorentz and polarization effects were also corrected. The structure of **1** was solved by the direct method with SHELXS-86[17] and by subsequent difference Fourier syntheses. The structure refinement with anisotropic parameters by the block-diagonal least-squares technique using UNICS III[16] was carried out for all non-hydrogen atoms. Atom-scattering factors were taken from Cromer and Waber.[18] Anomalous dispersion effects were included in F_{calc}.[19] Details of the crystallographic parameters are given in Table 1. Final positional parameters for **1** and the selected bond distances are listed in Tables 2 and 3, respectively. The labeling of atoms and the thermal vibrational ellipsoids for **1** are shown in Figure 2. The obtained *R* value is slightly larger than those reported for the other perovskites, presumably because of the poor crystallinity of **1**.

Ac magnetic susceptibility and dc magnetization were measured on a Lake Shore ACS7221 and Quantum Design MPMS-XL SQUID magnetometers. Variable-temperature measurements were carried out in the range 4−25 K. Field-dependent measurements were done in the field up to 1 T, after the sample was cooled under 0 external field.

3. Results and Discussion

Crystal Structure. The crystal structures of related compounds **2** and **3** were obtained in the previous study.[20] Their lattice parameters are listed in Table 4 in order to compare with those of **1**. The compounds **1** and **3** crystallize in the orthorhombic *Pbca* space group, while **2** crystallizes in the monoclinic $P2_1/c$ space group. Although **2** belongs to a different crystal system, the three compounds are isostructural. Figure 3 shows a schematic comparison between the unit cells of the two crystal systems, where the anilinium ions are omitted for the sake of clarity. The unit cell of **1** or **3** includes two organic−inorganic−organic sandwich layers, while that of **2** includes

Table 2. The Atomic Coordinates (×10000) and Equivalent Isotropic Thermal Parameters (100 Å) for **1**[a]

atom	*X*	*Y*	*Z*	$B_{eq}{}^b$
Cu	5000(0)	0(0)	5000(0)	2.5(0.1)
Br(1)	2335(2)	106(1)	2091(2)	3.3(0.1)
Br(2)	4815(3)	746(1)	5408(3)	3.7(0.1)
Cl	4454(11)	2534(2)	742(12)	7.2(0.3)
N	5069(25)	699(5)	−215(26)	4.8(0.6)
C(1)	4979(26)	1164(5)	40(28)	3.2(0.5)
C(2)	3744(29)	1383(6)	−1008(29)	3.5(0.6)
C(3)	3598(32)	1807(7)	−814(30)	4.5(0.7)
C(4)	5821(33)	1781(7)	1499(29)	4.3(0.7)
C(5)	4646(32)	2005(7)	476(34)	5.2(0.8)
C(6)	5993(33)	1352(8)	1315(31)	4.9(0.8)

[a] Estimated standard deviations in parentheses. [b] $B_{eq} = (8/3)\pi^2(U_{11}(aa^*)^2 + U_{22}(bb^*)^2 + U_{33}(cc^*)^2 + 2U_{12}aa^*bb^* \cos\gamma + 2U_{13}aa^*cc^* \cos\beta + 2U_{23}bb^*cc^* \cos\alpha)$.

Table 3. Selected Bond Distances (Å) and Angles (deg) for **1**[a]

	Distances		
Cu−Br(1)	2.437(2)	Br(1)−N	3.55(2)
Cu···Br(1)	3.069(2)	Br(2)−N	3.46(2)
Cu−Br(2)	2.419(2)		
	Angles		
Cu−Br(1)−Cu	164.6(1)	N−Br(2)−Cu	95.0(3)
Br(1)−Cu−Br(2)	89.7(1)	Br(1)−Cu···Br(1)	92.6(1)

[a] Estimated standard deviations in parentheses.

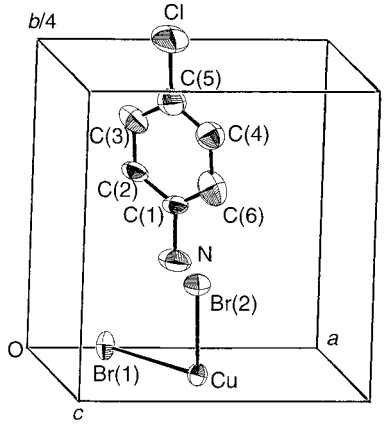

Figure 2. The labeling of atoms and the thermal vibrational ellipsoids for **1**.

Table 4. The Crystal Parameters Reported for **2** and **3**[a]

	2	**3**
formula	$C_{12}H_{14}N_2CuCl_6$	$C_{12}H_{14}N_4O_4CuCl_4$
fw	462.52	483.63
cryst syst	monoclinic	orthorhombic
space group	$P2_1/c$	*Pbca*
a/Å	16.436(4)	7.063(1)
b/Å	7.397(1)	32.460(6)
c/Å	7.265(1)	7.925(2)
β/deg	101.51(2)	
V/Å^3	865.5(3)	1816.9(6)
Z	2	4

[a] From ref 16.

(16) Sakurai, T.; Kobayashi, K. *Rikagaku Kenkyusho Hokoku* **1979**, *55*, 69.
(17) Sheldrick, G. M. Thesis, University of Goettingen, Germany, 1986.
(18) Cromer, D. T.; Waber, J. T. *International Tables for X-ray Crystallography*; The Kynoch Press: Birmingham, England, 1974.

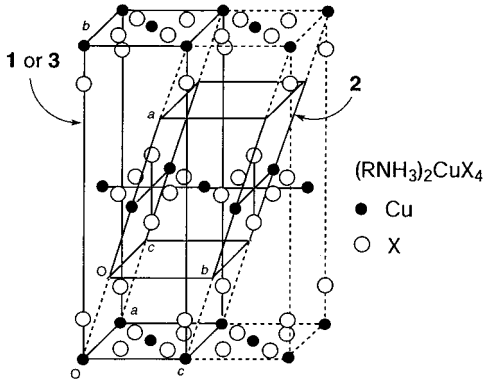

Figure 3. The schematic comparison between the unit cells of **1** or **3** and **2**.

Table 5. The Crystal Parameters Reported for **2** and **3**[a]

	1	**2**[b]	**3**[b]
D_L/Å[c]	3.069(2)	2.906(2)	3.075(2)
D_S/Å[c]	2.437(2)	2.309(2)	2.303(2)
interlayer distances/Å	16.041	16.105	16.230

[a] Estimated standard deviations in parentheses. [b] From ref 16. [c] D_L and D_S are defined in Figure 1.

one. The cell volume of **1** or **3** is twice as large as that of **2**. In Figure 4, parts a and b show side views of the layered structures in **1** and **2**, respectively. The alignments of the anilinium cations in the organic bilayer seem to cause the difference in crystal system. In the crystal of **2**, the neighboring layers A and B are related by an inversion center and, in addition, there is a 2-fold screw axis parallel to the *b* axis. In the crystal of **1**, there is no inversion center between A and B but they are related by a 2-fold screw axis operation parallel to the *c* axis. As a result, the molecular axes of the cations in the neighboring layers A and B appear parallel in **2**, while they are slightly tilted in **1**. It is worth noting that the two kinds of crystal systems have been observed in the $(RNH_3)_2CuCl_4$ series before.[1,18,20]

The structure of the copper halide layer is characterized by two kinds of copper−halide distances, the equatorial (D_S) and axial (D_L) distances caused by the Jahn−Teller effect. The values of D_S and D_L for **1**−**3** are listed in Table 5. The interlayer distances in the three are also shown there. D_S for **1** is longer than the values for **2** and **3**, probably because of the larger radius of the bromide ion. The value of D_L for **3** is larger than those for **1** and **2**, presumably due to a molecular arrangement distortion in the organic layer of **3**.[20] The observed values of D_S and D_L for **1**−**3** are typical for the layered copper chloride and bromide perovskites. Concerning the interlayer distances, there is no significant difference among the three.

Magnetic Properties. The magnetic properties of **1** and **2** have been investigated by Ishikawa et al. previously, by means of ac susceptibility and NQR measurements.[15] They reported that **1** and **2** showed long-range magnetic ordering at $T_N = 14$ and 9 K, respectively. The circles, triangles, and diamonds in Figure 5 represent the temperature dependence of χ_{ac} (real part) for **1**−**3**, which were re-examined in this work under an oscillating field (125 Hz) of 1−5 Oe in the temperature range 5−30 K on heating. The results obtained for **1** and **2** agree with the reported ones.[15] The materials **1**, **2**, and **3** exhibit magnetic ordering with an abrupt increase in χ_{ac} at 15, 9.1, and 7.0 K, respectively.

(19) Ibers, J. A.; Hamilton, W. C. *Acta Crystallogr.* **1964**, *17*, 781.
(20) Sekine, T.; Okuno, T.; Awaga, K. *Mol. Cryst. Liq. Cryst.* **1996**, *279*, 65.

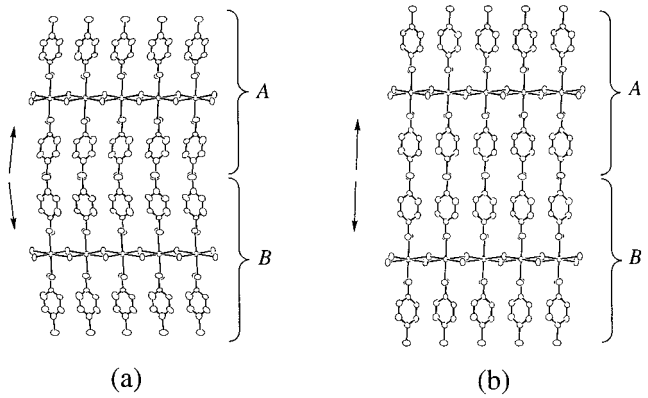

Figure 4. The side views of the layered structures for **1** (a) and **2** (b).

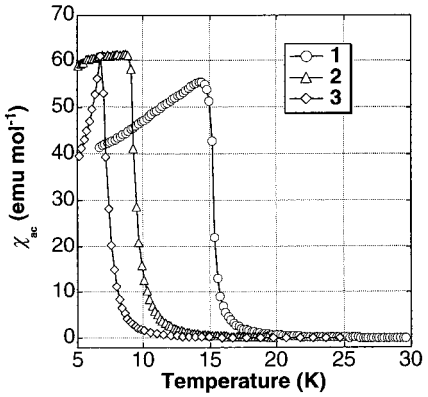

Figure 5. The temperature dependence of χ_{ac} for **1** (circles), **2** (triangles), and **3** (diamonds).

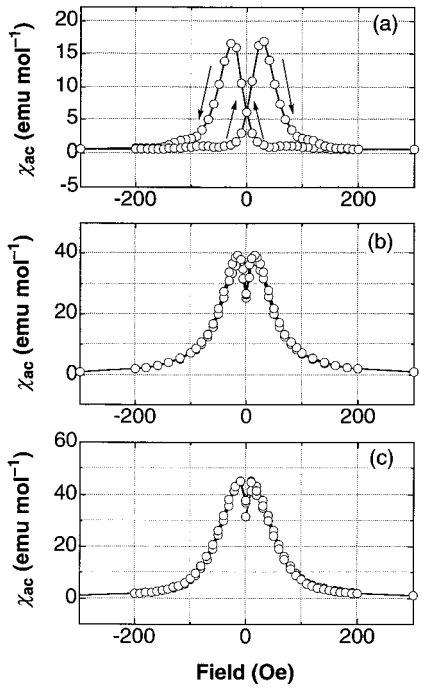

Figure 6. The field dependence of χ_{ac} for polycrystalline samples of **1** at 7 K (a), **2** at 6 K (b), and **3** at 5 K (c).

Figure 6a shows the magnetic field dependence of χ_{ac}, or namely the differential susceptibilities $(\partial M/\partial H)_T$, for a polycrystalline sample of **1** at 7 K. Upon increasing the magnetic field from 0, the plots have a maximum at 30 Oe, at which the magnetization curve has the largest gradient. After passing the maximum, χ_{ac} goes down to 0, showing saturation of the

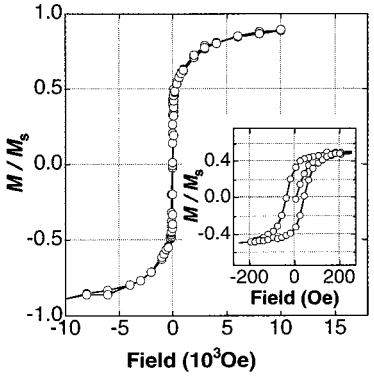

Figure 7. The $M-H$ curve for **1** measured at 7 K. The inset shows the behavior in the −250 to 250 Oe range on an enlarged scale.

magnetization. When the magnetic field is decreased, a maximum of χ_{ac} appears at −30 Oe. The behavior indicates a hysteresis loop of magnetization caused by the spontaneous magnetic moment at 7 K. Figure 7 shows the field dependence of M/M_S for **1** at 7 K, where M is the dc magnetization and M_S is the saturation magnetization. The inset shows the low-field behavior on an enlarged scale. The $M-H$ curve also shows a hysteresis loop, confirming the presence of the spontaneous magnetization. The magnitude of the remnant magnetization is 33% of the saturation magnetization.

The field dependencies of χ_{ac} for **2** and **3** are shown in Figure 6, parts b and c, respectively. The plots for each material also make two maximums at about −15 and 15 Oe, but no hysteresis is found. The absence of the hysteresis loop indicates that **2** and **3** are simple antiferromagnets composed of the intralayer ferromagnetic interaction and the interlayer antiferromagnetic interaction, as well as the other Cu(II) layered perovskites. The maximums in χ_{ac} would correspond to spin−flip transitions. It is concluded that the substitution of chloride with bromide for X in (*p*-chloroanilinium)$_2$CuX$_4$ leads to the occurrence of spontaneous magnetization. To our knowledge, this is the first experimental demonstration of the spontaneous magnetization in the Cu(II) layered perovskite materials.

The cause of the spontaneous magnetic moment in **1** would be explained by either ferromagnetism or canted ferromagnetism. If the interlayer magnetic coupling is ferromagnetic, the spins would be all aligned parallel and the magnetic system would be characterized in terms of simple 3D ferromagnetism. In this case, the spontaneous magnetization should be parallel to the easy axis. On the other hand, canted ferromagnetism would result from an anisotropic interlayer magnetic interaction, no matter whether it is ferromagnetic or antiferromagnetic. In the picture of the canted ferromagnetism, the spontaneous magnetization should be perpendicular to the easy axis. Since remnant magnetization of **1** is 33% of the saturation magnetization, neither the simple nor canted ferromagnetism can be excluded.

The field dependence of χ_{ac} for the single crystal of **1** was carefully examined, to clarify the mechanism. Figure 8a shows the results, when the magnetic field is applied parallel to the *b* axis at 5 K. The values of χ_{ac} show a hysteresis which is similar to that of the polycrystalline sample. Compound **1** behaves as a ferromagnet in the field parallel to the *b* axis. Figure 8b shows the data in the field parallel to the *a* axis. The plots make sharp peaks at 130 and −130 Oe, but no hysteresis is seen. Such peaks have been observed for $(C_2H_4NH_3)_2CuCl_4$ and have been attributed to the spin−flip transitions.[14] In general, the spin−flip transitions occur in the magnetic field parallel to the antiferromagnetically ordered spins. It is known that the

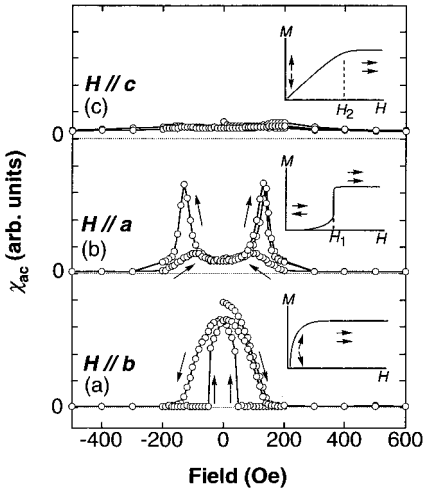

Figure 8. The field dependence of χ_{ac} for the single crystal of **1**, in the field parallel to the *b* axis (a), the *a* axis (b), and the *c* axis (c).

magnetic susceptibility parallel to the easy axis is nonzero and constant in the spin−flip phase but begins to decrease suddenly at a critical field, at which the transition from spin−flip phase to paramagnetic phase takes place. However, the plots of χ_{ac} for **1** make no plateau after the sharp peaks, suggesting the absence of the spin−flip phase. The sharp peaks of χ_{ac} would be due to metamagnetic transitions from the antiferromagnetic state to the paramagnetic state. This transition is usually realized under the condition that the magnetic anisotropy is larger than the antiferromagnetic coupling energy. It is concluded that compound **1** behaves as an antiferromagnet in the field parallel to the *a* axis. Figure 8c shows χ_{ac} along the *c* axis. The values of χ_{ac} are nonzero and depend little on the field. This strongly indicates that the *c* axis coincides with the magnetic hard axis. The single-crystal measurements for **1** indicate that the easy axis is the *a* axis and the direction of the spontaneous magnetization is parallel to the *b* axis. From the orthogonality between the easy axis and the spontaneous magnetization, canted ferromagnetism is reasonably concluded for the mechanism of the spontaneous magnetization in **1**. It is worth noting here that two-dimensional canted ferromagnetism has been observed in the manganese and iron layered perovskites.[21,22]

The insets in Figure 8, parts a, b, and c schematically show the alignments of "the magnetic moments" on two neighboring layers in **1** with increases in field parallel to the *b*, *a*, and *c* axes, respectively. Here, "the moment" means the intralayer magnetic moment summed by the intralayer ferromagnetic interaction. In the insets of Figure 8b,c, the spin canting toward the *b* axis is ignored. The expected shapes of the magnetization curves are also drawn there. The field dependence of χ_{ac} for **1** in Figure 8 indicates two critical fields, H_1 and H_2, whose definitions are shown in the insets. Now let us estimate the magnetic parameters for **1**, the interlayer exchange constant J' and the magnetic anisotropy field in the layer H_A^{in}, and compare them with those of other layered perovskites.[23,24] As shown in Figure 8b, the critical field, H_1, of the metamagnetic transition is 130 Oe at 5 K. We confirmed that the value of H_1 depended little on temperature within the experimental error in the range

(21) Groenendijk, H. A.; Duyneveldt, A. J. v.; Willett, R. D. *Physica* **1979**, *98B*, 53.
(22) Bloembergen, P.; Berkhout, P. J.; Franse, J. J. M. *Int. J. Magn.* **1973**, *4*, 219.
(23) Zhou, P.; Drumheller, J. E.; Patyal, B.; Willett, R. D. *Phys. Rev. B* **1992**, *45*, 12365.
(24) Yamazaki, H. *J. Phys. Soc. Jpn.* **1976**, *41*, 1911.

2−7 K and adopt it as the H_1 value at absolute 0. Since the antiferromagnetic interlayer exchange field, H_E, is equal to H_1, the J' value can be calculated according to the formula $H_E = 2z'J'S/g\mu_B$, where z' and g are the number of nearest neighbors and the g factor, respectively. Assuming that $z' = 2$ and $g = 2.0$, we obtain $J'/k_B = 0.01$ K. This is comparable to the values reported for the other $(RNH_3)_2CuBr_4$ materials[23] and for the $(RNH_3)_2CuCl_4$ series[24] but is much smaller than those for the $(NH_3C_nH_{2n}NH_3)CuBr_4$ series.[8] In the field parallel to the c axis, the magnetic moments are aligned parallel to the field above the critical field H_2 of 150 Oe. The H_2 value can be related to the anisotropy field in the layer, H_A^{in}. Since the metamagnetic transition has been observed instead of a spin−flip transition, $H_A^{in} > H_E$, but the value of H_2 indicates that the intensities of H_A^{in} and H_E are on the same order. The typical values of H_A^{in} for the $(RNH_3)_2CuCl_4$ series are in the range 50−100 Oe.[24] The value of H_A^{in} for **1** is not as extraordinary as that of a copper layered perovskite. We could not estimate the anisotropy field out of the layer, H_A^{out}, because the presence of spontaneous magnetization along the b axis prevented us from measuring the perpendicular susceptibility.

Here we discuss the origin of the spin canting in **1**. Since there is no single-ion anisotropy on the copper(II) ion ($S_{Cu} = {}^1/_2$), we take into account the antisymmetric spin coupling. The antisymmetrical part of an exchange interaction is the well-known Dzyaloshinsky−Moriya interaction that is the mechanism of canted ferromagnetism. The antisymmetrical part of a dipolar interaction can also be the reason for the spin canting.[25] The strongest interaction is the intralayer ferromagnetic one, but the 3D magnetic structure is governed by the following three minor factors: the isotropic antiferromagnetic exchange interaction between the layers, the magnetic anisotropy, and the antisymmetric parts of the spin couplings (exchange and dipolar interactions).[25] In the following discussion, "the moment" also means the intralayer magnetic moment. The energies of the isotropic antiferromagnetic exchange and the magnetic anisotropy term are minimized when the magnetic moments are aligned exactly antiparallel with each other. However, the energetical minimum of the antisymmetric term appears when the moments are perpendicular. The thermodynamic potential of such system studied by Dzyaloshinsky is well-established to possess double minimums with respect to the angle θ between the moments.[26] One minimum occurs at $\theta = \pi$, a completely antiparallel spin alignment, due to the isotropic exchange and the magnetic anisotropy; the other occurs at $\theta = \pi - \alpha$, a canted spin alignment, due to the antisymmetric term.

The spin canting is not allowed in **2** because the adjacent layers are related by a translational operation,[23] while the space group (*Pbca*) of **1** and **3** allows it. Although there is no symmetry difference between **1** and **3**, the canted ferromagnetism is not observed in **3**. Further, $(C_2H_5NH_3)_2CuCl_4$ also belongs to the same crystal system, but it has been reported not to show spontaneous magnetization.[22] The crystal structure of **1** has no extraordinary feature compared with those of other layered perovskites.

Next, let us pay attention to the electronic structures of **1**−**3**. Whether the spin structure prefers a simple antiferromagnetic alignment or a canted one depends on the balance of the antisymmetric term and the other terms. The antisymmetric parts of the magnetic exchange and dipolar interactions are related to the matrix elements of the spin−orbit interaction between the ground and excited states.[25] It is established that the interaction is stronger in the bromide compounds than in the chloride compounds.[23] In addition, the antisymmetric term is effectively enhanced, when the energy gap ΔE_1 between the ground state and the lowest excited state, which corresponds to that between the $d_{x^2-y^2}$ and d_{yz} (or d_{zx}) levels in this case, is small. The value of ΔE_1 in **1** is easily speculated to be smaller than that in **2** or **3**, because the interaction between the d_{xy} orbital on the Cu(II) ion and the $p\pi$ orbitals on the halide ions in **1** is much stronger than that in **2** or **3**.[27] Their colors reflect the differences in ΔE_1: the crystals of **1** appear dark violet in contrast to the yellow appearance of those of **2** or **3**, because of a red shift of the LMCT band in **1**. The lower LMCT transistion energy in **1** is due to the higher energy of $p\pi$ orbitals in the bromide ions, which raises the d_{yz} and d_{zx} orbital levels in the Cu(II) ion and results in the smaller ΔE_1 value in **1**. Therefore, it is expected that the antisymmetric term in **1** is stronger than those in the copper chloride compounds. It is possible that higher excited states, such as LMCT states, also contribute to the antisymmetric part, although it is hard to quantitatively estimate their contributions. As was explained before, the $(RNH_3)_2CuX_4$ series is considered to have a double minimum potential well with respect to the angle between the magnetic moments in the neighboring layers, caused by the competition among the isotropic interlayer antiferromagnetic interaction, the magnetic anisotropy, and the antisymmetric term. Since there is no structural factor which can explain the magnetic difference between **1** and **3**, the quantitative difference in the antisymmetric term would be responsible for the magnetic difference. The enhancement of the antisymmetric term would be the reason for the canted ferromagnetism in **1**.

4. Concluding Remarks

We have investigated the crystal structure and magnetic properties of **1**. The compound exhibits spontaneous magnetization, which is interpreted in terms of canted ferromagnetism. The enhancement of the spin−orbit interaction in **1** is suggested to be responsible for the spin canting.

Acknowledgment. This work was supported by the Grant-In-Aid for Scientific Research from the Ministry of Education, Science and Culture, of the Japanese Government, and by the CREST (Core Research for Evolution Science and Technology) of the Japan Science and Technology Corp. (JST).

Supporting Information Available: Summary of structure determination and solution refinement, list of anisotropic temperature factors, distances, angles, and stereoview for (p-Cl-anilinium)$_2CuBr_4$ (5 pages). Ordering information is given on any current masthead page.

IC970793Z

(25) Moriya, T. In *Magnetism*; Rado, G. T., Suhl, H., Eds.; 1963; Vol. 1, p 85.
(26) Dzyaloshinsky, I. *J. Phys. Chem. Solids* **1958**, *4*, 241.
(27) Huheey, J. E. *Inorganic chemistry*, 3rd ed.; Harper & Row: New York, 1983.